Hepatoprotective and anti-hyperplastic effects of silver nanoparticles biosynthesised using aqueous extracts of *M. scaber*: Insights from acetaminophen and testosterone experimental models

Temitayo I. Adesipe[1*] and *Abiodun* H. Adebayo[2]

[1]Department of Science Laboratory Technology, Federal Polytechnic Ilaro, Ogun state, Nigeria

[2]Department of Biochemistry,College of Science and Technology, Covenant University Ota, Ogun state, Nigeria

Abstract. Nanoparticle-based approaches have gained increasing attention due to their stability, bioavailability, and multifunctional biological activities. Aqueous extract of *Mitracarpus scaber* was utilized for silver nanoparticles (AgNPs) synthesis at an elevated temperature of 100oC following established protocol. Techniques including UV–visible (UV–vis) spectroscopy and Transmission electron microscopy (TEM) were used to analyze the synthesized AgNPs. The hepatoprotective and anti-hyperplastic potentials of the biosynthesized silver nanoparticles (Aq-AgNPs) was then evaluated using standard methods. The first indication of successful Aq-AgNPs synthesis was the color change from dark brown to light yellow observed after the addition of $AgNO_3$ solution to the aqueous extract of *Mitracarpus scabe*r. The UV spectrum of Aq-AgNPs was observed to be 419 nm which is characteristic of silver nanoparticles while TEM analysis revealed that the biosynthesized silver nanoparticles were predominantly spherical with an average size of 91.5 ± 35nm. The result of the hepatoprotective effect showed that Aq-AgNPs significantly reduced serum ALT ($p < 0.001$), creatinine ($p < 0.05$), urea ($p < 0.05$) and cholesterol levels ($p < 0.05$) of rats induced with liver damage, while enhancing antioxidant defenses (GSH, and SOD) and decreasing lipid peroxidation (MDA) in them. The result of the anti-hyperplastic activity revealed that the administration of Aq-AgNPs markedly lowered interleukin-6 ($p < 0.0001$), prostate weight ($p < 0.001$), MDA levels ($p < 0.001$) and PSA ($p < 0.05$) which were comparable to Finasteride. On the other hand, histological examinations revealed that treatment with Aq-AgNPs reversed alterations produced by acetaminophen and testosterone in the liver and prostate gland respectively. These findings indicates the potential of biosynthesized AgNPs using aqueous extract of *Mitracarpus scaber* as a novel therapeutic strategy for managing liver injury and benign prostatic hyperplasia.

* Corresponding author:iyanu.adesipe@federalpolyilaro.edu.ng

1 Introduction

The liver is a key metabolic organ that controls systemic homeostasis, including the metabolism of steroid hormones, detoxification, and the removal of xenobiotics. Because of its vulnerability to drug-induced toxicity, pharmaceutical therapies must focus on it [1]. Overdosing on acetaminophen, or paracetamol, is a common experimental model of hepatocellular injury and continues to be one of the primary causes of acute liver failure globally. Hepatic function is eventually hampered by the pathophysiology, which includes oxidative stress, inflammation, and excessive production of reactive metabolites. Thus, it is highly relevant to biomedicine to find new hepatoprotective medicines that can lessen these consequences [2]. On the other hand, components of seminal fluid secreted by the prostate, an androgen-dependent male accessory gland, are essential to reproductive function. BPH is the outcome of unchecked prostatic development caused by age-related hormonal changes, including those involving testosterone and its strong metabolite dihydrotestosterone (DHT). In order to assess pharmaceutical compounds with anti-hyperplastic potential, testosterone-induced BPH models in rodents have been thoroughly verified [3,4].

Despite having distinct physiological functions, the liver and prostate are connected via endocrine and metabolic pathways. While the liver regulates circulating sex hormones, which in turn impact prostatic growth, prostatic disease can result in systemic oxidative and inflammatory mediators that might impair hepatic function. This link emphasises the medicinal potential of compounds that target redox balance and hormone control in a number of organ systems [5-7].

In this context, plant-derived nanomedicine presents special opportunities. Silver nanoparticles synthesised using *M. scabe*r at ambient temperature have been reported for their synergistic antioxidant, anti-inflammatory, and hormone-modulatory activities [8,9]. The current study examines the hepatoprotective and anti-hyperplastic effects of silver nanoparticles synthesized using *Mitracarpus scabe*r at an elevated temperature of 100 ^{o}C.

2 Materials and methods

For this experiment, only analytical-grade chemicals were used.

2.1 Biosynthesis of silver nanoparticles

After making a 0.1M $AgNO_3$ solution, 90 ml of the solution was put into a flask containing 10 ml of an aqueous *Mitracapus scaber* extract. The mixture was incubated at 100 °C while being constantly stirred. The resulting AgNPs were then centrifuged for 20 minutes at 6000 rpm. The centrifuged pellets were repeatedly rinsed with distilled water to remove any remaining silver ions and other undesirable elements. The resulting biosynthesised silver nanoparticles were designated Aq-AgNPs [9].

2.2 Characterization

The silver nanoparticles (Aq-AgNPs) created in this investigation were examined as described by Mahboob, [10]. The samples' absorption spectra were detected at wavelengths ranging from 200 to 700 nm utilising UV-visible spectrophotometer (Agilent Technologies). It was verified that silver nanoparticles were formed by observing the absorption peak. Also. the hydrodynamic size distributions and polydispersity index (PDI) of nanoparticles were

analyzed by using dynamic light scattering (DLS) technique which was performed on a Zetasizer instrument (DLS; Zetasize Nano-ZS; Malvern Instruments, UK) at 25 °C. DLS quantifies light scattering intensity dynamic variations created by particle brownian motion to determine particle velocity distribution. Based on particle distributions, the software estimates mean particle diameter and the polydispersity index (PdI) shows the solution's size range. Monodisperse states are 0 on the PdI scale, while polydisperse states are 1.

2.3 Animals/Ethical approval

A cohort of 35 Wistar rats (weighing between 150-200 g) was sourced from the Laboratory Animal House of the College of Medicine, University of Lagos, located in Idi-araba, Lagos state, Nigeria. The study was approved by the Animal ethics committee of the Federal Polytechnic Ilaro. The experiments were conducted in accordance with the institutional Animal Ethics Committee guidelines as well as the ARRIVE recommendations and the National Institute of Health (NIH) guidelines for the treatment of laboratory animals [11].

2.4 Evaluation of anti-hyperplastic effect of biosynthesized silver nanoparticles

2.4.1 Experimental Design

The anti-hyperplastic effect of thermal assisted synthesized silver nanoparticles using *M. scaber* (Aq-AgNPs) were assessed in rats induced with Benign prostatic hyperplasia in a fourteen days experimental period, the rats were initially divided into four groups of five. A subcutaneous injection of testosterone propionate (TP) at a dose of 3 mg/kg/bw was administered into rats to cause Benign prostatic hyperplasia while 50 mg/kg and 5mg/kg/day of Aq-AgNPs and finasteride were administered orally respectively to the rats alleviate benign prostatic hyperplasia [12] .
The design of the experiment used is as follows:
• **Group 1:** The control group consisted of rats that were not given any test samples neither were they induced with benign prostatic hyperplasia. A single dosage of distilled water (vehicle, 1 mL) was given to them orally every day.
• **Group 2:** This group's rats were given a daily single dose of 3 mg/kg/bw testosterone propionate (TP) only to induce benign prostatic hyperplasia.
• **Group 3**: This group's rats were given a daily single dose of 3 mg/kg/bw testosterone propionate (TP) to induce benign prostatic hyperplasia and 50 mg/kg /bw of thermally aided synthesised silver nanoparticles using *Mitracarpus scaber* aqueous extract.
• **Group 4:** These rats were given a daily single dose of 3 mg/kg/bw testosterone propionate (TP) to induce benign prostatic hyperplasia and 5 mg/kg/bw of finasteride.

2.5 Evaluation of hepatoprotective effect of biosynthesized silver nanoparticles

2.5.1 Experimental design

The hepatoprotective effect of thermal assisted synthesized silver nanoparticles using *M. scaber* (Aq-AgNPs) were assessed in rats induced with liver damage in a seven days experimental period following the method described by Obiora et al., [13] with little modifications. The rats were initially divided into three groups of five animals each and then

a single oral dose of acetaminophen (ASAP) at 500 mg/kg/bw was given to rats to cause liver damage while 50 mg/kg and 5mg/kg/day of Aq-AgNPs was administered orally respectively to the rats alleviate liver damage.
The design of the experiment used is as follows:
• **Group 1:** The control group consisted of rats that were not given any test samples neither were they induced with liver damage. A single dosage of distilled water (vehicle, 1 mL) was given to them orally every day.
• **Group 2:** This group's rats were given a single oral dose of 500 mg/kg/bw acetaminophen (ASAP) only to induce liver damage.
• **Group 3:** This group's rats were given a daily single daily dose at 50 mg/kg of thermally aided synthesised silver nanoparticles using *Mitracarpus scaber* aqueous extract.

2.6 Biochemical analysis

Rats in the different experimental set up were euthanized by cervical dislocation on the day following the last dose of medications. Prior to this, blood samples were collected from the medial canthus of the animals' eye. Serum was obtained by centrifuging the blood samples at 3000 rpm for 10 minutes after allowing them to coagulate at room temperature for 30 minutes. For the experimental set up involving determination of anti hyperplastic activity, the clear sera was used to estimate the levels of free prostate serum albumin (PSA), interleukin-6 (IL-6), alanine transminase (ALT) and creatinine as well as malondialdehyde (MDA), glutathione (GSH) and superoxide dismutase (SOD) levels while the clear sera gotten from the blood of the animals in the experimental set up involving determination of hepatoprotective activity were utilised for ALT, creatinine, urea and cholesterol levels determination as well as MDA, GSH, and SOD levels. The prostate glands of rats in the former experimental set up were surgically removed and carefully weighed while the liver organ of rats in the later experimental set up was also removed. The different organs were preserved without delay in 10% formal saline prior to histological analysis.

2.6.1 Serum prostate- specific antigen estimation

The serum concentrations of free PSA were assessed using commercially available Bio-inteco free PSA test kits (TOSOH India Pvt. Ltd.) following the manufacturer's instructions on an automated immunoassay analyzer.

2.6.2 Serum analysis of IL-6 cytokine

IL-6 cytokine level from rats' serum samples were evaluated using the immunoassay biomarkers® ELISA method-based immunoassay biomarkers. Using an LT 4500 microplate reader, the experiment was carried out as directed by the manufacturer.

2.6.3 Assessment of liver function

Using commercially available diagnostic kits from Biosystems S.A. Costa Brava, Barcelona (Spain), serum levels of alanine aminotransferase (ALT), creatinine, urea and cholesterol were determined according to the manufacturer's instructions.

2.6.4 Assessment of tissue oxidative stress markers

Malondialdehyde was measured with the thiobarbituric reacting substances (TBARs) test as a lipid peroxidation indicator [14] while reduced glutathione (GSH) was measured in serum samples [15]. The yellow complex containing molybdate and H_2O_2 formed the basis of the test. Superoxide dismutase (SOD) activity was measured by using the method of Misra and Fridovich [16].

2.7 Histology

The prostate and liver sample were preserved in solutions of neutral buffered formalin, underwent a series of procedures, and were then enclosed in paraffin blocks. The tissue samples were sliced into sections with a thickness of five micrometres and then stained using hematoxylin and eosin. The slides were analyzed using a microscope to observe any histoarchitectural alterations [12].

2.8 Statistical analysis

Results were presented as mean ± SEM and analyzed using ANOVA and Dunnett's multiple comparison tests, with a single pooled variance. The ANOVA test was conducted with GraphPad Prism 6.0. P-values < 0.05 were considered statistically significant.

3 RESULT

3.1 Characterization of biosynthesised silver nanoparticles

3.1.1 UV–Visible spectroscopy and TEM Image

The outcome of the UV–visible and TEM analysis of biosynthesised silver nanoparticles (Aq-AgNPs) is disclosed in Fig. 1A and B below. The spectra comprise absorption peak within electromagnetic spectrum's visual range. Successful silver nanoparticles' formation was indicated by the detection of an absorption peak of 419 nm (Fig. 1A) while the analysis of the TEM image revealed irregular shaped particles with an average size of 91.15 ± 35 nm (Fig. 1B).

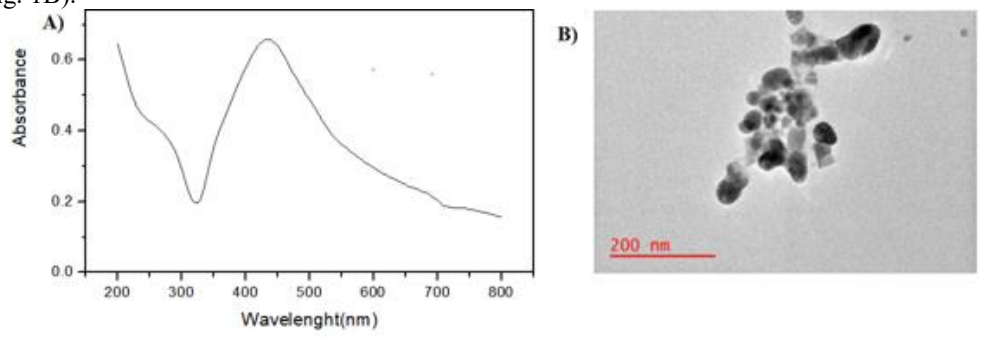

Fig. 1. A) Spectra of UV-VIS absorbance and B) TEM Image of Aq-AgNPs

3.1.2 Dynamic light scattering technique(DLS)

DLS analysis was performed to determine the mean hydrodynamic diameter (Z-average) and PDI value for estimating the size of Aq-AgNPs in colloidal suspension as well as their dispersion respectively. The result of this analysis is shown in Table 1 below.

Table1. Hydrodynamic diameter (Z-average) and PDI value of Aq-AgNPs

Plant Extract	$AgNO_3$ concentration	Extract ratio to silver nitrate	Color	Z-Average size (nm)	PDI
M. Scaber **aqueous extract**	0.1M	1:9	Light Yellow	227.9	0.590

3.2 Evaluation of anti-hyperplastic effect of biosynthesized silver nanoparticles (Aq-AgNPs)

3.2.1 Effect of Aq-AgNPs on prostate weight, IL-6 Cytokine, MDA and PSA levels of rats induced with BPH

The effect of Aq-AgNPs on prostate weight, IL-6 Cytokine, MDA and PSA levels of rats induced with BPH is shown in Fig. 2 (A-D). Changes and distribution in prostate weight of animals at the experiment's expiration is shown in Fig. 2A. Administration of Aq-AgNPs significantly ($P<0.001$) reduced the prostate weight, however no significant ($p > 0.05$) reduction was observed in the group administered with finasteride. The results pertaining to serum IL-6 cytokines, MDA and PSA levels in the study groups are illustrated in Fig. 2 (B-D). In contrast to the testosterone propionate (TP) induced BPH model group, which exhibited exceptionally high IL-6 cytokine, MDA and PSA concentrations, the treatment group supplemented with Aq-AgNPs as well as finasteride demonstrated statistically significant reduction ($P<0.0001$, $P<0.001$) in IL-6 cytokine and MDA levels, respectively (Fig. 2 B,C). The highest significant ($P<0.001$) reduction in the average PSA concentration was observed in the group that received finasteride, followed by the group that received Aq-AgNPs ($p < 0.05$) (Fig. 2 D).

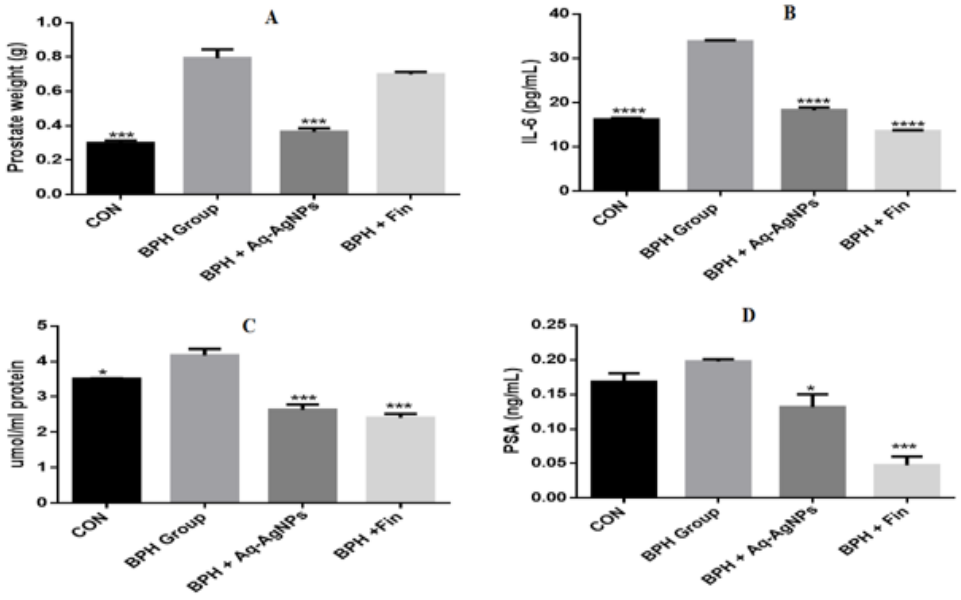

Fig. 2. Effect of biosynthesised silver nanoparticles on A) prostate weight, B) IL-6 Cytokine, C) MDA and D) PSA levels of rats induced with BPH. CON- Control, BPH group- Benign prostatic hyperplasia group, BPH+Aq-AgNPs- Thermally assisted AgNPs of *M. scaber* aqueous extract, Fin- Finesteride. Bars indicates mean ± SEM for n=3. When comparing treated individual groups to BPH group,*P < 0.05 shows a significant decrease in level, **P < 0.01 shows a very significant decrease in level, ***P<0.001 indicates a more significant decrease in level, ****P<0.0001 indicate an extremely significant decrease in level.SEM; Standard error of mean.

3.2.2 Effect of Aq-AgNPs on glutathione (GSH) superoxide dismutase (SOD) and catalase (CAT) levels of rats induced with BPH

The effect of Aq-AgNPs on glutathione (GSH), superoxide dismutase (SOD) and catalase (CAT) levels of rats induced with BPH is shown in Fig. 3 (A-C). The concentrations of GSH were markedly increased ($P < 0.01$, $P < 0.05$) in groups treated with finasteride and group treated with Aq-AgNPs respectively, however no signicant increase ($p > 0.05$) in SOD level was observed in both groups in comparison to the induced group. Furthermore, only the treatments involving finasteride exhibited a significant increase ($P < 0.001$) in catalase.

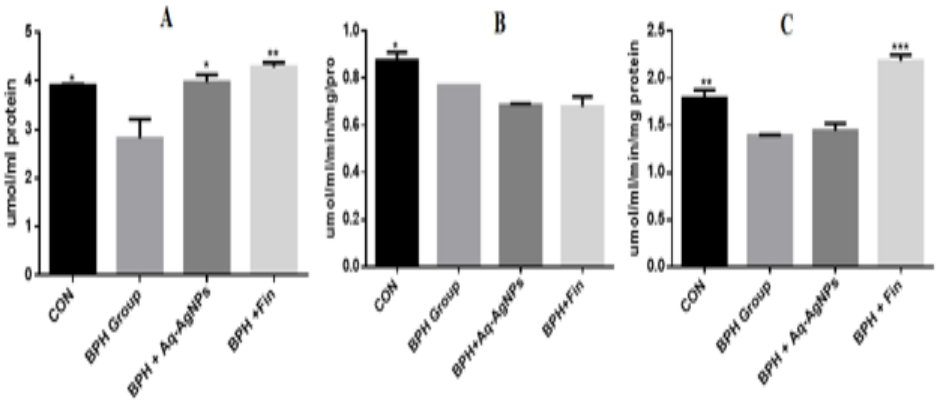

Fig. 3. Effect of Aq-AgNPs on A) GSH, B) SOD and C) CAT levels of rats induced with BPH. CON- Control, BPH group- Benign prostatic hyperplasia group, BPH+ Aq-AgNPs- Thermally assisted AgNPs of *M. scabe*r aqueous extract, Fin- Finesteride. Bars indicates mean ± SEM for n=3. When comparing treated individual groups to BPH group,*P < 0.05 shows a significant increase in level, **P < 0.01 shows a very significant increase in level, ***P<0.001 indicates a more significant increase in level. SEM; Standard error of mean.

3.2.3 Effect of Aq-AgNPs on aspartate aminotransferase (ALT) and creatinine levels of rats induced with BPH

The effect of Aq-AgNPs on aspartate aminotransferase (ALT) and creatinine levels of rats induced with BPH is shown in Fig. 4 A, B. In contrast to the testosterone propionate (TP) induced BPH model group, which exhibited exceptionally high ALT and creatinine levels, ALT level was significantly (P<0.0001, P<0.001) reduced in the treatment groups supplemented with Aq-AgNPs and finasteride, respectively (Fig. 4 A). The highest significant (P<0.01) reduction in creatinine level was observed in the group that received Aq-AgNPs, followed by the group that received finasteride (p < 0.05) (Fig. 4 B).

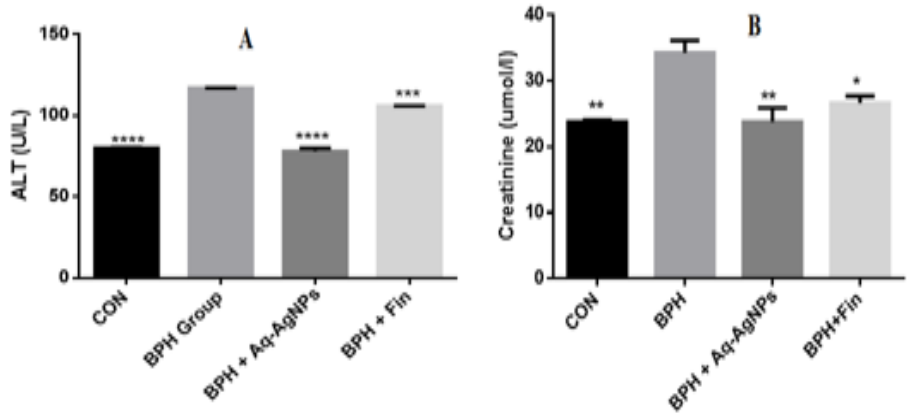

Fig. 4. Effect of Aq-AgNPs on ALT and creatinine levels of rats induced with BPH. CON- Control, BPH group- Benign prostatic hyperplasia group, BPH+Aq-AgNPs- Thermally assisted AgNPs of *M. scaber* aqueous extract, Fin- Finesteride. Bars indicates mean ± SEM for n=3. When comparing treated individual groups to BPH group,*P < 0.05 shows a significant decrease in level, **P < 0.01 shows a very significant decrease in level, ***P<0.001 indicates a more significant decrease in level.****P<0.0001 indicate an extremely significant decrease in level. SEM; Standard error of mean.SEM; Standard error of mean.

3.2.4 Histopathology of prostate tissue

The histological study in Fig. 5 A, B, C, D depicts the normal control group, BPH group, group treated with Aq-AgNPs (BPH+Aq-AgNPs) and group treated with finasteride (BPH+Fin), respectively. The prostate epithelium of the normal control group show prostatic glands lined by cuboidal to columnar epithelium which form luminal papilliform projections in areas with the glands indicating interglandular smooth muscle fibres, corpora amylacea were also seen within the lumen of cellular acini gland; no abnormalities were seen (Fig. 5 A). The effectiveness of the technique, duration and materials employed to induce BPH in rats in this study is demonstrated by sample images of BPH group prostate tissue (Fig. 5 B). The photomicrograph reveals prostatic glands lined by proliferative epithelial cellular elements of the prostate, leading to an enlarged prostate gland forming a thickened lining of the affected acini (hyperplasia), increased number of epithelial and stromal cells in the periurethral area of the prostate which is characteristics of benign prostatic hyperplasia. However, sample images of prostate tissues of the group with treated with Aq-AgNPs and finasteride showed benign prostatic hyperplasia histological pattern regression (Fig. 5 C, D respectively).

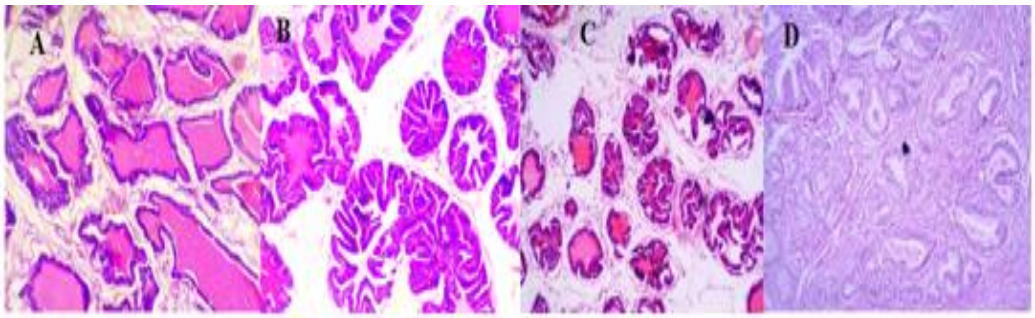

Fig. 5. Sample images of prostate tissues stained with H&E (magnifcation×100) of; A (Normal Control), B (BPH Group), C (BPH+ Aq-AgNPs), D (BPH+ Finesteride)

3.3 Evaluation of hepatoprotective effect of biosynthesized silver nanoparticles

3.3.1 Effect of Aq-AgNPs on serum biochemical markers of rats induced with liver damage

The effect of Aq-AgNPs serum biochemical markers of rats induced with liver damage is shown in Fig. 6 (A-E). Administration of Aq-AgNPs resulted in significant reductions ($P<0.01$, $P<0.0001$, $p < 0.05$, $p < 0.05$, $P<0.01$) of MDA, ALT, urea, creatinine and cholesterol levels, respectively in comparison to the induced group.

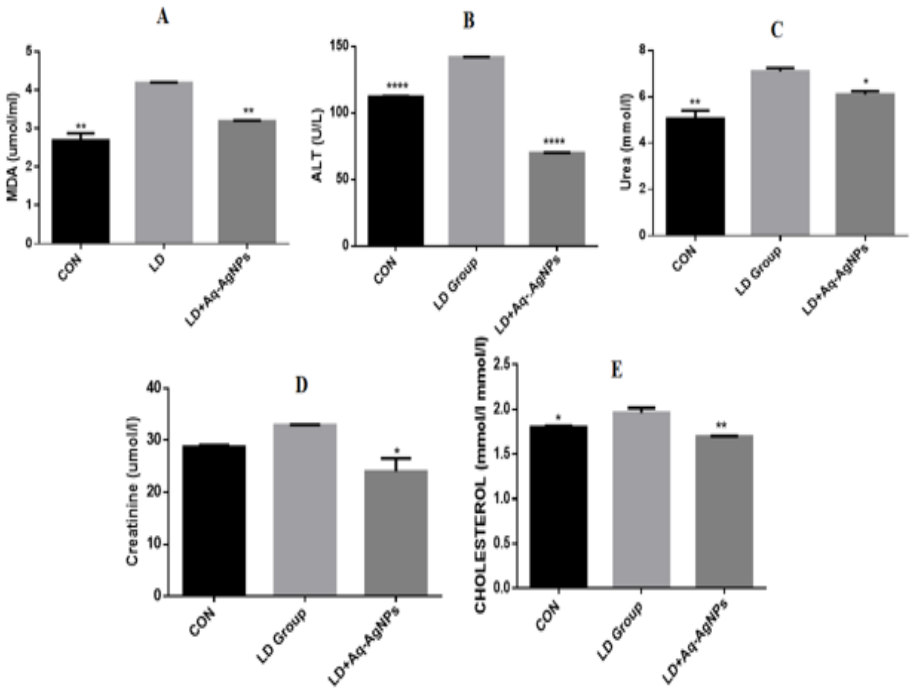

Fig. 6. Effect of Aq-AgNPs on Serum Biochemical Markers of rats induced with liver damage. CON-Control, LD group- Liver damage group, LD+Aq-AgNPs- Thermally assisted AgNPs of *M. scabe*r aqueous extract. Bars indicates mean ± SEM for n=3. When comparing treated individual groups to LD group,*P < 0.05 shows a significant decrease in level, **P < 0.01 shows a very significant decrease in level, ****P<0.0001 indicate an extremely significant decrease in level. SEM; Standard error of mean.

3.3.2 Effect of Aq-AgNPs on antioxidant enzyme levels of rats induced with liver damage

The effect of Aq-AgNPs on antioxidant enzyme levels of rats induced with liver damage is shown in Fig. 7 A, B. Administration of Aq-AgNPs resulted in significant increase ($p < 0.05$) in GSH and SOD levels. However no signicant increase ($p > 0.05$) was observed in catalase level in comparison to the induced group.

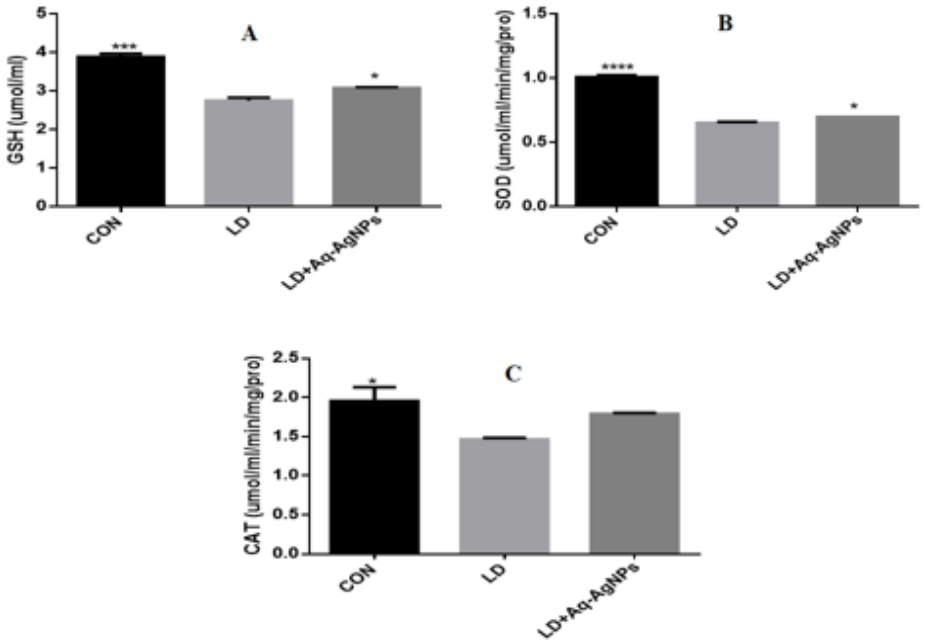

Fig. 7. Effect of Aq-AgNPs on A) GSH, B) SOD C) CAT levels of rats induced with liver damage.CON- Control, LD group- Liver damage group, LD+Aq-AgNPs- Thermally assisted AgNPs of *M. scaber* aqueous extract. Bars indicates mean ± SEM for n=3. When comparing treated individual groups to LD group,*P < 0.05 shows a significant increase in level, ****P<0.0001 indicate an extremely significant increase in level. SEM; Standard error of mean.

3.3.3 Histopathology of Liver Tissue

The histological study in Figure 8 A, B, C depicts the normal control group, LD group and group treated with Aq-AgNPs (LD+Aq-AgNPs), respectively. The histologic section of the normal liver tissue show parallel radially arranged plates of hepatocytes with central vein (CV), portal vein (PV) and the basophilic portion with nucleus and the acidophilic cytoplasm of the acinar cells. No abnormalities are seen.(Fig. 8 A). The effectiveness of the technique, duration and materials employed to induce liver damage in rats in this study is demonstrated by sample image of the liver tissue of the liver damage group (Fig. 8 B). The photomicrograph show parallel radially arranged plates of hepatocytes, with the portal space and periportal zone filled with floccular pink fluid material common with edema, congested aggregates of red blood cells also seen, both of which are strong indicators of liver damage. However, sample image of liver tissue of the group with treated with Aq-AgNPs showed liver damage histological pattern regression (Fig. 8 C).

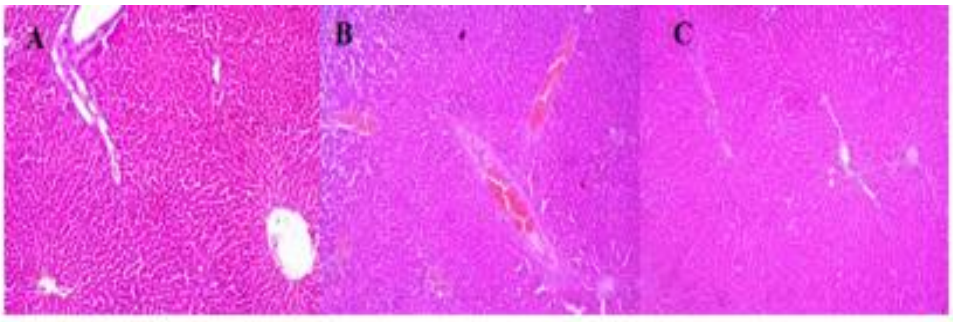

Fig. 8. Sample images of liver tissues stained with H&E (magnifcation×100) of; A(Normal Control), B (Liver damage Group), C (Liver damage + Aq-AgNPs)

4 DISCUSSION

The current work demonstrates the anti-hyperplastic and hepatoprotective properties of thermally assisted silver nanoparticles biosynthesised utilising *Mitracarpus scaber* aqueous extract (Aq-AgNPs). Metallic AgNPs' formation was verified by checking the distinct absorption band of silver nanoparticles in the UV-Vis spectrum, which occurred at 300–800 nm wavelength. The AgNPs synthesised with *M. scaber* aqueous extract displayed a maximal absorbance peak at 419 nm in the surface plasmon resonance band. Similar peaks have been reported in literature [17]. TEM analysis revealed irregular particles with average sizes of 91.15 ± 35 nm (Fig. 3B), however DLS analysis revealed larger hydrodynamic diameter (227.9 nm) and a PDI value of 0.590 for the biosynthesized silver nanoparticles (Aq-AgNPs) .This is because unlike microscopy, dynamic light scattering (DLS) approach does not enable the assessment of individual particles' size within aggregates. Thus, in many instances, the hydrodynamic radius measured using the DLS technique is significantly bigger than the particle dimensions reported by TEM [18].

In the testosterone propionate (TP)-induced BPH model, Aq-AgNPs significantly decreased prostate weight (Fig. 2A), in contrast to finasteride, which had no discernible impact. Additionally, Aq-AgNPs dramatically decreased MDA, PSA, and IL-6 cytokine levels (Fig. 2B–D), demonstrating their anti-inflammatory and antioxidant properties. Aq-AgNPs continued to be efficacious even though finasteride resulted in the most noticeable lowering of PSA, indicating that their protective function might go beyond androgen-dependent mechanisms. A selective antioxidant mechanism is implied by the fact that Aq-AgNPs increased GSH levels (Fig. 3A) but did not significantly raise SOD or catalase (Fig. 3B–C). Significantly, Aq-AgNPs reduced creatinine more effectively than finasteride (Fig. 4B), indicating additional renoprotective advantages. The reduction of hyperplastic characteristics was further supported by histological findings (Fig. 5C), which were consistent with biochemical results.

In the acetaminophen-induced liver damage model, Aq-AgNPs significantly lowered serum ALT, urea, creatinine, cholesterol, and MDA levels (Fig. 6A–E) while restoring antioxidant defenses via elevated GSH and SOD (Fig. 7A–B). Histopathology (Fig. 8C) revealed restoration of normal hepatic architecture with reduced edema and congestion compared to

untreated liver-damaged rats (Fig. 8B). These findings demonstrate a strong hepatoprotective effect, likely mediated through attenuation of oxidative stress and reinforcement of endogenous antioxidant systems, particularly the glutathione pathway [19].

Collectively, Aq-AgNPs demonstrated superior efficacy over finasteride in reducing prostate weight and creatinine levels, in addition to exhibiting robust hepatoprotection. Their ability to simultaneously modulate oxidative stress, suppress inflammatory cytokines, and restore organ integrity underscores the therapeutic potential of green-synthesized nanoparticles.

5 CONCLUSION

Given their dual protective roles, Aq-AgNPs synthesized using *Mitracarpus scaber* aqueous extract at 100 °C may provide a multifunctional platform for the management of oxidative stress and inflammation-associated disorders.

References

1. S. S. Qadri, D. Javaid, A. Reyaz, S. Y. Ganie, and M. S. Reshi, Liver disorders and phytotherapy, Toxicol. Rep. **14**, 102047 (2025). https://doi.org/10.1016/j.toxrep.2025.102047
2. R. Li, H. Wu, Y. Xu, X. Xu, Y. Xu, H. Huang, and H. Li, Underlying mechanisms and treatment of acetaminophen-induced liver injury," Mol. Med. Rep. **31**, 106 (2025). https://doi.org/10.3892/mmr.2025.13471
3. D. Marcoccia, M. Mollari, F. S. Galli, C. Cuva, V. Tassinari, and A. Mantovani, Prostate as a target of endocrine disrupting chemicals: relevance, pathways, assays," Reprod. Toxicol. **133**, 108867 (2025). https://doi.org/ 10.1016/j.reprotox.2025.108867
4. F. Hoseinpour, M. Hashemnia, H. Cheraghi, M. M. Salari Asl, F. Zare, and I. A. Zanjani, Protective effect of the hydroethanolic extract of camelthorn on benign prostatic hyperplasia induced by testosterone in rats, BMC Complement. Med. Ther. **25**, 136 (2025). https://doi.org/10.1186/s12906-025-04862-6
5. F. Zhang and W. Li, Impact of fatty liver index and metabolic dysfunction-associated steatotic liver disease on the risk of benign prostatic hyperplasia in older male adults," BMC Geriatr. **25**, 625 (2025). https://doi.org/10.1186/s12877-025-06314-9
6. M. Hassan, T. W. Flanagan, A. M. Eshaq, O. K. Altamimi, H. Altalag, M. Alsharif, and M. Megahed, Reduction of prostate cancer risk: role of frequent ejaculation-associated mechanisms, Cancers **17**, 843 (2025). https://doi.org/10.3390/cancers17050843
7. A. Kasarinaite, M. Sinton, P. T. Saunders, and D. C. Hay, The influence of sex hormones in liver function and disease, Cells **12**, 1604 (2023). https://doi.org/ 10.3390/cells12121604
8. T. I. Adesipe, A. Adebayo, and E. Iweala, Biosynthesis of silver nanoparticles using *Mitracarpus scaber* extracts for the treatment of infectious disease: synthesis, characterization, antibacterial and anti-inflammatory efficacy, Babcock Univ. Med. J. **7**, 160 (2024). https://doi.org/ 10.38029/babcockuniv.med.j..v7i1.428
9. T. I. Adesipe, E. J. Iweala, I. O. Ishola, O. A. Arotiba, and A. H. Adebayo, Utilizing *Mitracarpus scaber* extracts for green synthesis of silver nanoparticles: exploring physicochemical properties and chemopreventive activity against N-methylnitrosourea-

induced prostate carcinoma in rats, Nano-Struct. Nano-Objects **40**, 101363 (2024). https://doi.org/10.1016/j.nanoso.2024.101363

10. A. Mahboob, Analyses of biosynthesized silver nanoparticles produced from strawberry fruit pomace extracts in terms of biocompatibility, cytotoxicity, antioxidant ability, photodegradation, and in-silico studies, J. King Saud Univ. Sci. **34**, 102327 (2022). https://doi.org/10.1016/j.jksus.2022.102327
11. National Institute of Health Office of Animal Care and Use, Animal research advisory committee guidelines, (NIH, 2016). https://oacu.oir.nih.gov/animal-research-advisory-committee-guidelines
12. A. Ajayi et al., Biogenic synthesis of silver nanoparticles with bitter leaf aqueous extract and its effects on testosterone-induced benign prostatic hyperplasia in Wistar rat, Chem. Afr. **4**, 791 (2021). https://doi.org/10.1007/s42250-021-00272-6
13. O. F. Obiora, J. Bege, I. J. Agat, and N. J. Barnabas, Crude extracts of *Mitracarpus scaber* roots significantly ameliorate paracetamol-induced liver damage in rats, Am. J. Biomed. Life Sci. **7**, 148 (2019). https://doi.org/10.11648/j.ajbls.20190706.14
14. E. Nagababu, J. M. Rifkind, S. Boindala, and L. Nakka, Assessment of antioxidant activity of eugenol in vitro and in vivo, Methods Mol. Biol. **610**, 165 (2010). 10.1007/978-1-60327-029-8_10
15. D. J. Jollow, J. R. Mitchell, N. A. Zampaglione, and J. R. Gillette, Bromobenzene-induced liver necrosis: protective role of glutathione and evidence for 3,4-bromobenzene oxide as the hepatotoxic metabolite, Pharmacol. **11**, 151 (1974). https://doi.org/10.1159/000136485
16. H. P. Misra and I. Fridovich, The role of superoxide anion in the autooxidation of epinephrine and a simple assay for superoxide dismutase, J. Biol. Chem. **247**, 3170 (1972). https://doi.org/10.1016/S0021-9258(19)45228-9.
17. S. Dandapat, R. Srivastava, and M. P. S. Sinha, Impact of silver nanoparticles synthesized using aqueous extract of *Ganoderma applanatum* on thyroid and lipid parameters of albino rat, An. Biol. **43**, 139 (2021). http://dx.doi.org/10.6018/analesbio.43.14
18. S. K. Filippov, R. Khusnutdinov, A. Murmiliuk, W. Inam, L. Y. Zakharova, H. Zhang, and V. V. Khutoryanskiy, Dynamic light scattering and transmission electron microscopy in drug delivery: a roadmap for correct characterization of nanoparticles and interpretation of results, Mater. Horiz. **10**, 5354 (2023). https://doi.org/10.1039/D3MH00717K.
19. H. Jaeschke and A. Ramachandran, Oxidant stress and lipid peroxidation in acetaminophen hepatotoxicity, React. Oxyg. Species (Apex) **5**, 145 (2018). https://pmc.ncbi.nlm.nih.gov/articles/PMC5903282/